CHAPTER II

X-RAY DIFFRACTION STUDIES ON MESOGENIC SUBSTANCES: THEORETICAL BACKGROUNDS AND EXPERIMENTAL TECHNIQUES.

2.1.1. Classification of liquid crystals and their structures:

In section 1.1, we mentioned that thermotropic liquid crystals were broadly divided into three groups, viz., nematics, cholesterics and smectics. To date classification of different liquid crystal phases rests mainly on the work of Sackmann and his co-workers[1] which was based on the miscibility study. The miscibility rule states that if two liquid crystals are miscible in all proportions, they belong to the same class. The optical properties (textures and optical anisotropy) were also taken into consideration in this classification system. A. de Vries[2], afterwards, modified this classification system on the basis of miscibility relation, microscopic textures and X-ray diffraction patterns. Details of these classification systems and structures can be had from the review articles of de Vries[3], S.E.B. Petrie[4], J. Doucet[5], L.V.Azaroff[6] and Gray et al.[7,8]. From these it would be evident that lots of controversies are still going on about the structures of different phases. Without going into these controversies, we shall give the generally accepted views about the different liquid crystalline phases.

Nematic phases (N)

We have mentioned earlier that in nematic phases the long axes of the constituent molecules do have a preferred direction of orientation called the director ($\vec{n}$) but the molecular centres of mass are randomly distributed

as exist in conventional liquid. Because of the orientational order about $\vec{n}$ a nematic is a uniaxial medium with optical axis along $\vec{n}$. In all known cases there appears to be complete rotational symmetry around the axis $\vec{n}$. The direction of $\vec{n}$ is arbitrary in space and the states of the director $\vec{n}$ and $-\vec{n}$ are indistinguishable. Also nematic phases occur only with materials which donot distinguish between right and left; either each constituent molecule must be identical to its mirror image or, if it is not, the system must be a racemic mixture of the right and left handed species. From a crystallographic point of view the symmetry in nematics can be described by $D_{\infty h}$ in the Schonflies notation[10]. de Vries[9], however, observed another type of nematic phase called skewed cybotactic nematic (N_{SC}), where the molecules are arranged in small groups in such a way that they are parallel to each other with the centres of mass of the molecules in a fairly well defined plane and normal to the plane makes certain considerable angle with the molecular long axes. Since, as stated earlier, cholestarics are nothing but 'twisted' or 'chiral' nematics, de Vries[2] also proposed two types of cholesteric phases - ordinary nematic cholesteric(Ch_N)and layered or smectic cholesteric(Ch_S).

Smectic phases

The rigid-rod-like molecules, believed to be the building blocks of all liquid crystals, can array themselves in parallel layers to form a smectic mesophase.

The molecules may be normal to the planes of the layers or tilted within them. They may be randomly distributed within the layers or partly ordered or, in some cases, they form a two dimensional lattice within the layers. There can exist correlations between the layers but, except in more ordered ones, there are none. These lead to the possibility of a large number of smectic polymorphism and already as many as eleven smectic phases have been identified and designated as S_A, S_B, S_C, S_D, S_E, S_F, S_G, S'_G, S_H, S_K and S_J, S'_H, and S_I.

In most smectic phases the molecules are mobile in two directions and can rotate about one axis. The inter layer attractions are weak compared to the lateral forces between the molecules and the layers are able to slide over one another relatively easily. Consequently, the smectic phases have fluid properties, but are much more viscous than the other mesophases.

Smectic A phase (S_A)

This is the least ordered of all the smectic mesophases. Within the layers of S_A the long axes of the molecules lie parallel to one another, their direction being normal to the plane of the layer. The molecules are free to rotate about their long axes and the distribution of centre of mass of the molecules within the

layers is random[11-13]. Thus the layers have a low degree of order, each layer being ~ a two dimensional liquid. The layer thickness is, in most cases, close to the full molecular length. The molecular arrangement is shown in Fig.2.1. de Vries[14,15] now seems to believe that the molecules are tilted in S_A phase since the orientational order parameter (Sec. 2.2.2) in S_A is less than unity[14] and the layer thickness is less than the molecular length[3a]. It may also be mentioned here that new ~ results have emerged in the last few years concerning the existence of re-entrant nematic and smectic phases, bilayer-monolayer transitions, undulation structures and coexistent density waves of incommensurate wavelengths[16-27].

Smectic C phase (S_C)

The structure of S_C phase is similar to that of the S_A phase except that the long axes of the molecules are tilted with respect to the planes of the layers (Fig.2.1) and so layer spacing in S_C is less than that in S_A phase. S_C phase always occure at lower temperatures than the S_A phase in a sequence. Till angle of the S_C phase may be temperature dependent but, for most cases, it is temperature independent. Depending mainly upon the temperature dependence of tilt angle attempts have been made to divide S_C phase in three sub-groups[28].

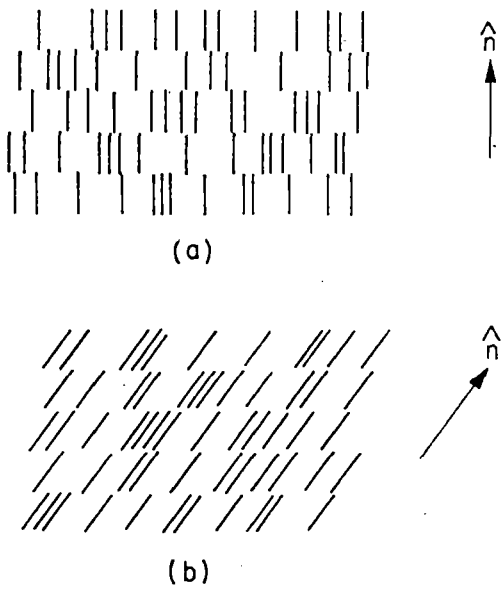

Fig.2.1 Schematic representation of two types of smectic order: (a) smectic A order; (b) smectic C order.

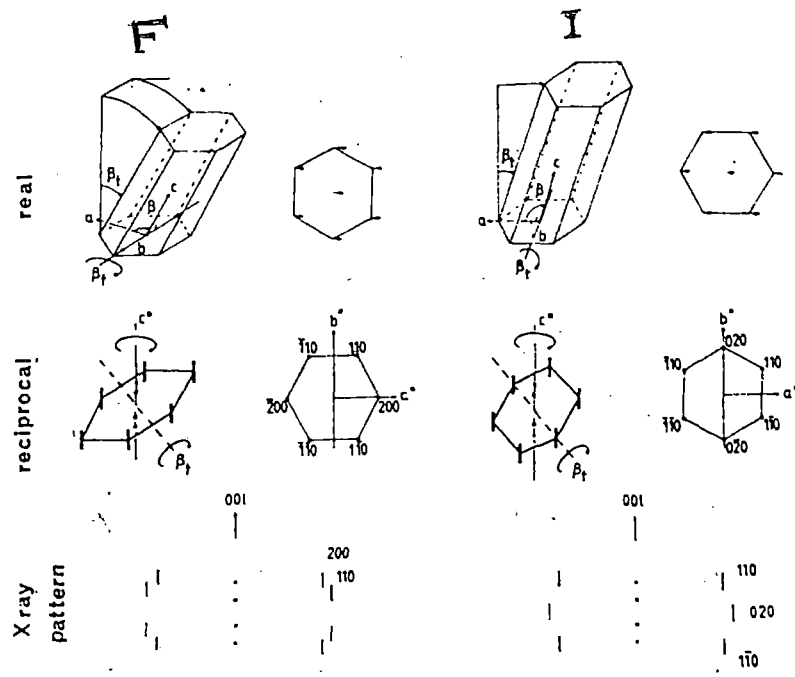

Fig.2.2 representation of real and reciprocal lattice for S_F and S_I phases and the resultant diffraction pattern as shown in Fig.2.10 and 2.11. The molecules are parallel to c and the pseudo-hexagonal packing of the molecules in the plane perpendicular to c is shown, with arrows indicating the direction of tilt. The hexagonal hko net is shown together with a perspective view depicting the tilt geometry and the diffuse bars of scattering parallel to c*. A schematic representation is given of the X-ray diffraction pattern with the beam parallel to the layers for a sample with disorder about c*.

Smectic D phase (S_D)

S_D mesophase possesses a cubic arrangement of spherical micelles and would appear to be an exception to the rule that all smectic structures have well defined stratification. In a number of compounds it occurs above S_C phase and some times below S_A[29-30].

Smectic F and Smectic I phases (S_F and S_I)

The structures of S_F and S_I phases have been determined very recently by Leadbetter group[31] (S_F) and Sackmann group[32] (S_I) and the relation between the two is also established by Leadbetter and his co-workers[33]. Both the phases consist of uncorrelated layers (at best correlation between 1 or 2 layers) in which the molecules are tilted relative to the layer normal and have limited positional correlations (about 30 molecular diameters) within layers. Both of them have three dimensional long range 'bond orientational order'[34] of the C-centred monoclinic lattices. They differ in the direction of the tilt of the molecules relative to the pseudo-hexagonal packing in the plane normal to the long axes: in S_F the tilt is directed towards an edge of the hexagon, while in S_I it is directed towards an apex as shown in Fig. 2.2.

Smectic B phase (S_B)

The molecules in S_B phase are also arranged in layers with the long axes normal to the layer planes. Within the layers, the molecular centres of mass are arranged in hexagonal symmetry (Fig. 2.3). In general the local structure is a herring bone packing and the average hexagonal symmetry is obtained by superposition of three different orientations of the local orthorhombic cells[33]. The situation is dynamic and individual molecules rotate[35,36] among six equivalent sites on a time scale of 10^{-11} s. The hexagonal layers have a bilayer stacking sequence of the form ABAB..... with molecular centres at (0,0) for A and at (2a/3, b/3) for B where a and b are basic hexagonal lattice vectors[37]. Trilayer ABCA....., random ABC....., highly disordered monolayer AA..... packing or no interlayer correlations are also reported[36]. In addition there is a crystal B-phase having long range 3-d order, of course, with considerable orientational disorder of the molecules.

Smectic E phase (S_E)

The S_E modification is a layered structure with a level of order more closely approaching to that of the crystalline state[29, 38,39] than that observed for even S_B. Doucet et al[38] concluded that the long axes of the molecules in S_E phase are normal to the layers. It was concluded that within the layers the molecules have a chevron structure with orthorhombic symmetry. Correlations of the orthorhombic array were also observed to exist over several

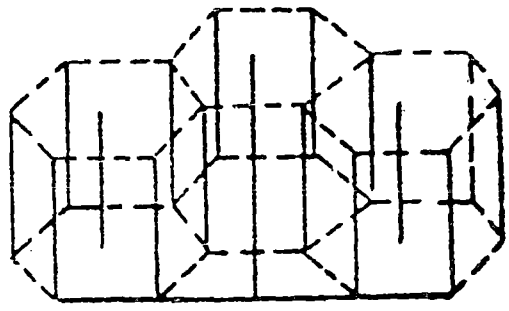

(a)

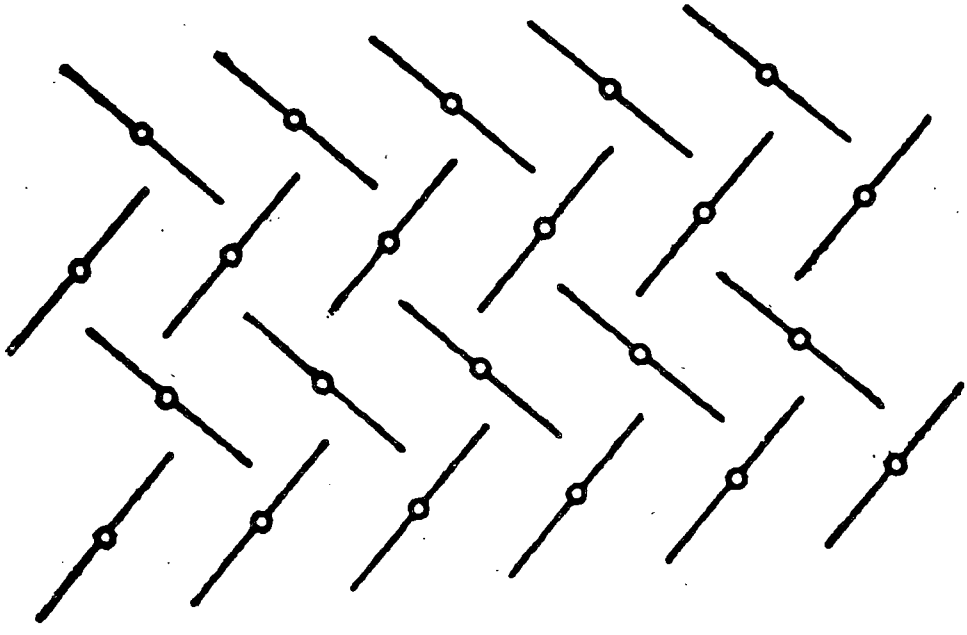

(b)

Fig. 2.3 a) Schematic representation of Smectic structure. b) Hexagonal herringbone packing as seen along the long axes of the molecules. The lines indicate the orientation of the molecular planes and circles mark the positions of the molecular axes; the circles form a hexagonal array.

layers, the arrangement being monolayer or bilayer for different substances. So the structure is considerably three-dimensional[40,41]. However, there is also considerable disorder because of vibration or libration, if not complete rotation, of the molecules around the molecular axes[42].

Smectic G, Smectic H, Smectic G' and Smectic H' phases- (S_G, S_H, S'_G and S'_H)

All these smectic phases have long range three-dimensional order[33] in the form of monolayer arrangement with considerable dynamic disorder. The S_G phase has a C-centred monoclinic cell with pseudo-hexagonal packing of the molecules within the layers and the molecules are tilted towards an edge of the hexagon as shown in Fig.2.2. In S_H phase the hexagon become more distorted and the cell is no longer C-centred as a result of a quenching of the 6-fold rotational disorder of the molecules which exists in S_G. The S_G phase certainly has rotational disorder in which the molecules reorientate[36] about their long axes on a time scale of 10^{-11} S while this is partially quenched in S_H phases[43,44].

The S'_G phase was first described by Doucet et al. for HOBACBC[45] and S'_H phase along with S'_G was found for 8OSF[31]. P.A.C. Gane et al.[33] first showed that S'_G and S'_H differ from S_G and S_H phases only in the tilt direction of the molecules. In these cases the molecules are tilted towards an apex of the pseudo-hexagonal molecular packing. Thus the molecular tilt in S_G and S_H phases

correspond to the tilt in S_E phase while that of S'_G and S'_H phases correspond to S_I phase.

Though the smectic phases E, G, H, G' and H' have long range three-dimentional order like the solid phase still they may be identified as liquid crystals because of the following reasons:

1. There is considerable orientational disorder of the molecules.
2. Possess fluidity
3. These phase transitions exhibit no supercooling effect whereas phase transition involving solid phases almost always show considerable supercooling.
4. The mosaic texturesof these phases strongly resembles those of S_B phase.
5. Mössbauer study[46] showed the solid phase to be 'decidedly more rigid' than the supercooled S_G phase at the same temperature.
6. A crystal structure of an optically active compound has a long range 3-d lattice just like any other crystal structure, but the lattice of a 3-d smectic phase becomes twisted if the molecules are optically active.

The assignment of the symbols to the different phase types was simply done in the order in which those phase types were discovered. We have, however, described

the phases not maintaining the alphabetical order but in accordance with the increasing orderness of the molecules in the phases. The sequence of the liquid crystalline state as indicated by observed variants is as follows:

Crystal S_H S_G S_E S_B S_F S_I S_C S_D S_A N Ch Isotropic

S'_H S'_G

Yet Smectic E and G modifications have not been observed in one compound and so their respective order is not verified. But since orthogonal phases are less ordered than the tilted ones, we have written S_E before S_G. All other sequences have been verified.

2.1.2. Methods of identification of different liquid crystalline phases:

As mentioned earlier identification of different phases and the corresponding transition temperatures can be made from miscibility study, mixroscopic texture and optical anisotropy study under a polarising microscope and from X-ray diffraction study. But transition temperatures can be measured most accurately by Differential scanning calorimetry ~~(sssc)~~ (DSC) or Differential thermal analysis (DTA) since by these methods even small changes in thermodynamic quantities (e.g. Enthalpy or Entropy)at

transition points can be detected which sometimes may go undetected[47] by optical study and the temperature range of a particular phase may be so small that X-ray diffraction study could not be made. Again from miscibility and optical microscopic studies a preliminary identification of the phases can be made. But to know the structural features of mesomorphic phases X-ray diffraction study is the most powerful tool at hand.

X-ray pattern of an unaligned liquid crystals consists of one or more inner ■ rings and one or more outer rings. The inner rings correspond to the molecular length (in case of nematics) or layer spacings (in case of smectics) and the outer rings are the characteristics of the lateral distribution of parallel molecules[9,3]. In aligned samples we get meridional and equatorial diffraction maxima ■■ as points or crescents. Characteristics of X-ray diffraction photographs and textures of different phases which we have used while identidying them are given in Table 2.1.

Table 2.1

Modifications	Optical properties	Texture	X-ray pattern for	
			unaligned samples	aligned samples
(1)	(2)	(3)	(4)	(5)
Ordinary Nematic	Uniaxially positive	Schlieren, threaded, marbled, homogeneous or pseudoisotropic.	Single diffuse inner ring and single diffuse outer ring (Fig.2.4)	Inner ring or crescent and outer crescents or diffuse ring with two maxima(Fig. 2.5).
Cybotactic nematic	Biaxial	-do-	-do- Only intensity of inner ring is far greater than that of the outer ring(Fig.2.6)	Four symmetrical inner spots along with outer crescents (Fig.2.7)
Nematic cholesteric	Uniaxially negative or isotropic, optically active.	Focal conic, ganddjean steps, homogeneous or isotropic	Same as ordinary nematic	Same as ordinary nematic.

Contd.....

Table 2.1. (Contd....)

(1)	(2)	(3)	(4)	(5)
Smectic cholesteric.	Biaxial	Focal conic or gandjeun steps.	-do-	-do-
Smectic A	Uniaxially positive.	Focal conic, fan shaped, polygonal, stepped droplets, homogeneous ring, pseudoisotropic.	Sharp inner ring(s) and one diffuse outer ring.	Sharp inner ring(s) or spots(s) and outer crescents or diffuse ring with two maxima. Lines through inner and outer maxima points are orthogonal (Fig. 2.8).
Smectic C	Biaxially positive.	Broken focal conic, schlieren or homogeneous.	Same as S_A	Same as S_A. Only lines through the inner spots and and outer maxima points are are non-orthogonal (Fig. 2.9)
Smectic F	Biaxially positive	Chequerboard, broken fan or schlieren.	Same as S_C. Only outer ring is comparatively less diffuse.	1st. and 2nd. order inner spots and one sharp outer ring with four symmetrical spots (Fig. 2.2 and 2.10).
Smectic I	-do-	-do-	-do-	1st. or 2nd. order inner spots and three symmetrical outer spots (Fig.2.2 and 2.11).

Contd.....

Table 2.1. (Contd...)

(1)	(2)	(3)	(4)	(5)
Smectic D	Isotropic	Isotropic mosaic or mosaic.	Same as nematic.	The inner ring splits up into six spots in an approximately hexagonal arrangement (Fig. 2.12).
Smectic E	Uniaxially positive.	Mosaic, stepped drops, homogeneous, pseudo-isotropic, schlieren.	One sharp inner ring and one sharp outer ring.	Sharp inner ring or spots, sharp outer ring with six maxima points or two symmetrical bars(Fig.2.13).
Smectic F	Uniaxially positive.	Mosaic or pseudoisotropic (Platelet)	Two or more sharp inner rings and three or more sharp outer rings(Fig.2.14).	2nd. or more order inner spots and second order outer spots in hexagonal symmetry.

Contd.....

Table 2.1 (Contd...)

(1)	(2)	(3)	(4)	(5)
Smectic G	Positive Biaxial.	Mosaic texture.	Two or more closely spaced outer rings. (Fig. 2.15).	Second or more order inner and outer ring set or spots (tilt like S_F).
Smectic H	-do-	-do-	-do-	Same as S_G only more distorted outer spots.
Smectic G'	-do-	-do-	Same as S_G	Second or more order inner and outer spots (tilt like S_I).
Smectic H'	-do-	-do-	-do-	Same as S'_G. Only more distorted outer spots.

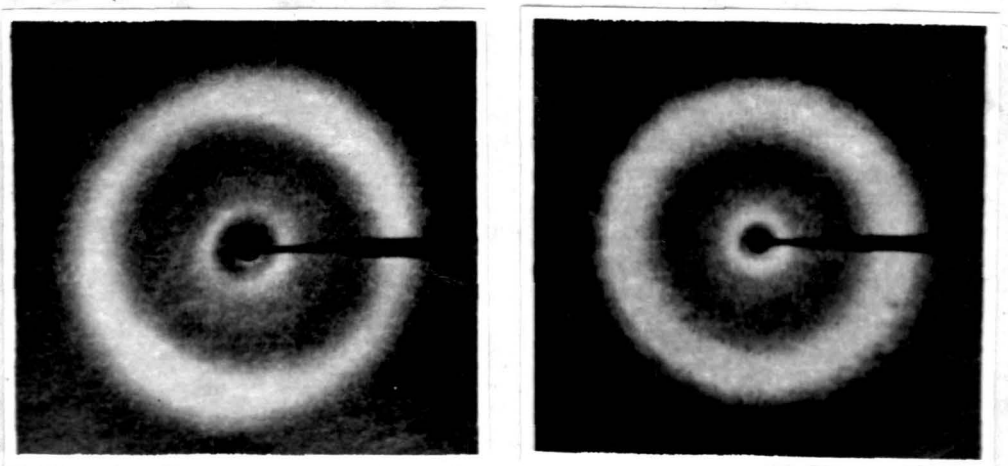

(a) (b)

Fig. 2.4(a) Powder photograph of ordinary nematic (N_O) phase.[2]
(b) Photograph of isotropic liquid phase.[2]

Fig. 2.5 Aligned photograph of ordinary nematic (N_O) phase.[2]

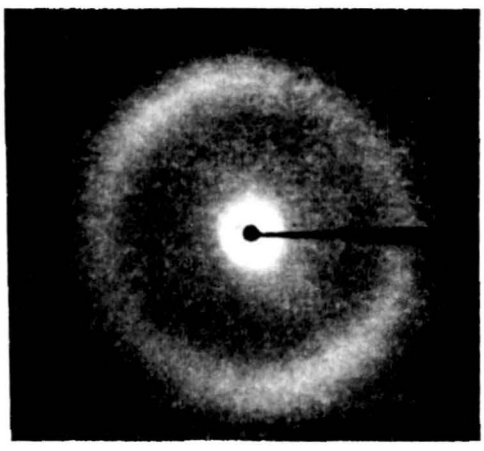

Fig. 2.6 Powder photograph of cybotactic nematic phase.[2]

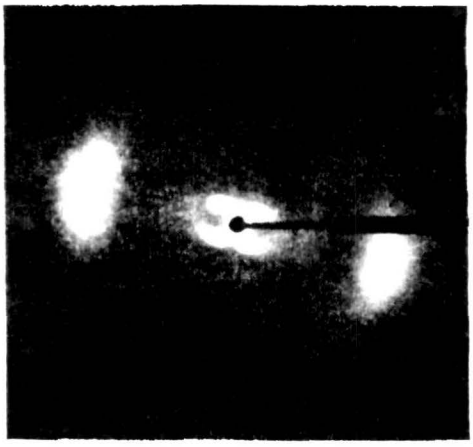

Fig. 2.7 Aligned photograph of Cybotactic nematic phase.[2]

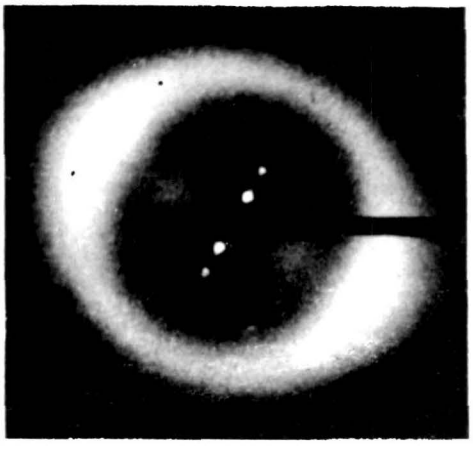

Fig. 2.8 Aligned photograph of Smectic A phase.[2]

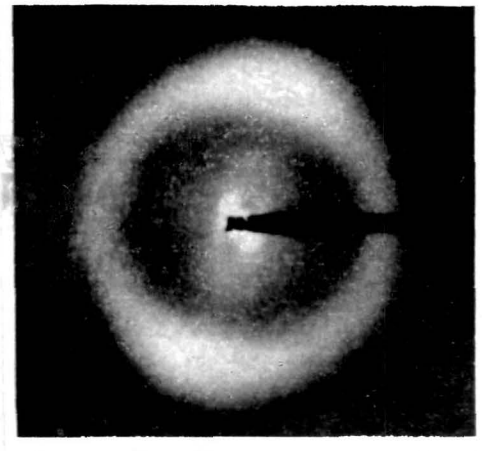

Fig. 2.9 Aligned photograph of Smectic C phase.[2]

Fig. 2.10 Aligned photograph of Smectic F phase.[33]

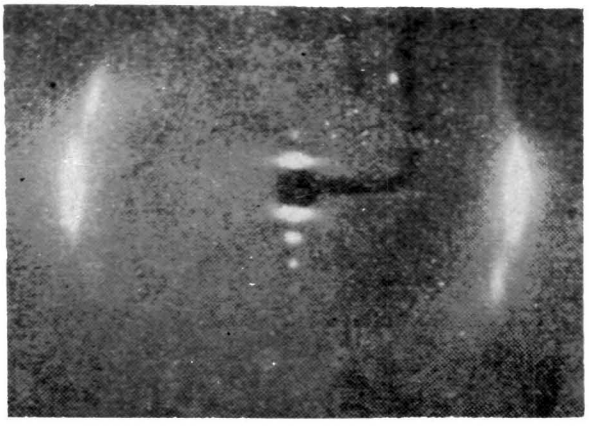

Fig. 2.11 Aligned photograph of Smectic I phase.[33]

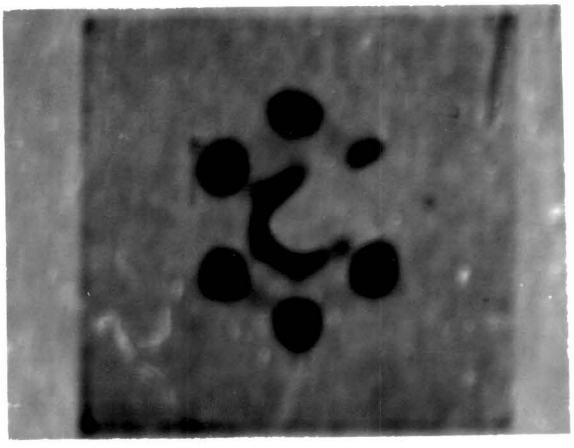

Fig. 2.12 Aligned photograph of Smectic D phase.[2]

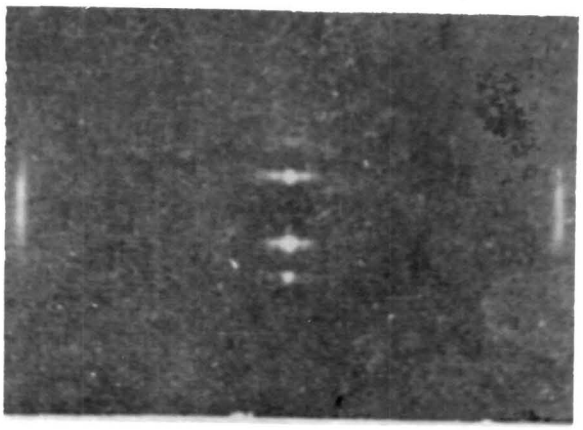

Fig. 2.13 Aligned photograph of Smectic B phase.[33]

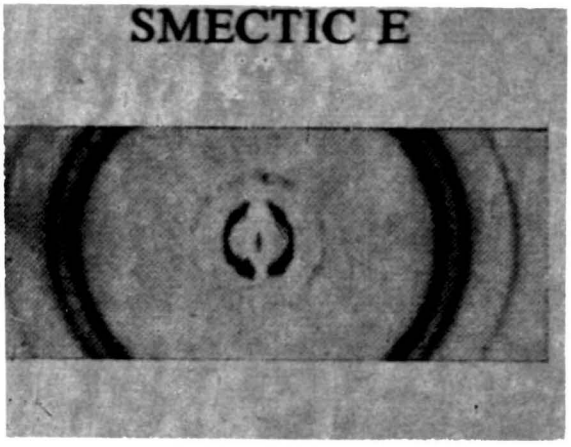

Fig. 2.14 Powder photograph of Smectic E phase.[2]

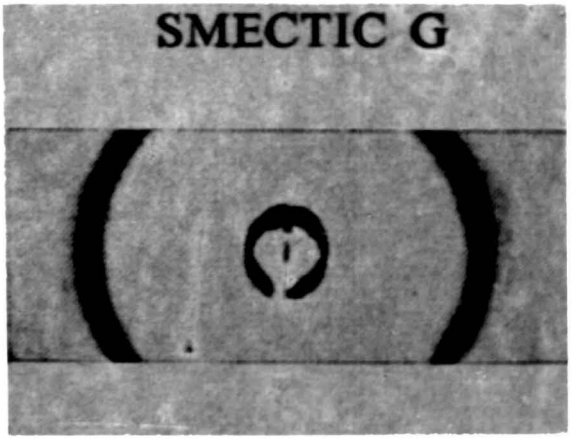

Fig. 2.15 Powder photograph of Smectic G phase.[2]

2.2.1. Theory of Nematic liquid crystalline state:

It has already been stated that the nematic liquid crystals differ from isotropic liquid by a long range orientational order of the long axes of the rod like molecules. The nematic phase has a lower symmetry than the high temperature isotropic liquid. We express this qualitatively by saying that the nematic phase is more ordered. To put this on a quantitative basis, we need to define an order parameter which is non-zero in the nematic phase but vanishes in the isotropic phase. The orientational potential energy of a molecule in the nematic liquid can be expressed in terms of this order parameter. Such an expression is given in the mean field theory of nematic liquid crystals. Once this is accomplished expressions for the orientational molecular distribution function are derived and the thermodynamic functions simply calculated. The character of the transformation from nematic liquid crystal to isotropic fluid is then revealed by the theory.

2.2.2. Order parameter:

In nematics the long axes of the molecules do have a preferred direction of orientation called the director $\vec{n}$. Assuming the molecules as rigid rods, the orientation of a particular molecule with respect to the director $\vec{n}$ (taken to be the Z-direction) can be completely

defined by three Eulerian angles θ , ϕ and ψ (Fig.2.16). Due to thermal energy the individual molecules or small group of molecules fluctuate but the director may be taken as the most probable direction. It is mentioned earlier that the director $\vec{n}$ and $-\vec{n}$ are equivalent and the molecules are cylindrically symmetric. But in practice none of the above assumptions are strictly valid i.e. the molecules are flexible to some extent, there are cases where the heads and tails are distinguishable[48] and the molecules are more lath like than cylindrical[49]. However, the deviation from the idealised case is small and the molecules are often assumed to rotate freely around the long molecular axes. Because of the cylindrical symmetry no order would exist for ϕ and ψ and under the most simplified consideration θ becomes the only parameter to characterise the orientational ordering. However θ is not itself a convenient order parameter and also by analogy with ferromagnetism we cannot take $\cos\theta$ as the natural order parameter because here $\vec{n}$ and $-\vec{n}$ are equivalent. Taking these into consideration, the scalar order parameter for the nematic phase is defined as

$$\langle P_2 \rangle = \tfrac{1}{2}\left(3\langle \cos^2\theta \rangle - 1\right) \qquad \ldots(2.1)$$

The average is taken over all the molecules. The expression we have chosen for order parameter is second order Legendre polynomial. For a perfectly ordered sample all $\theta = 0$ and

$\langle \cos^2\theta \rangle$ = 1 so that $\langle P_2 \rangle$ = 1 whereas when all the molecules are randomly oriented (i.e. isotropic liquid) $\langle \cos^2\theta \rangle = 1/3$ and $\langle P_2 \rangle$ = 0. In the nematic phase it has an intermediate value which decreases with temperature and drop abruptly to zero at the nematic isotropic point T_{NI}.

2.2.3. Molecular Mean Field Theory of Nematic Crystals:

An approach that has proved to be extremely useful in developing a theory of spontaneous long range orientational order and the related properties of the nematic phase is the molecular field method closely analogous to that introduced by Weiss in ferromagnetism. Each molecule is assumed to be in an average orientating field due to its environment but otherwise uncorrelated with its neighbours. The first molecular field theory of the nematic state was proposed in 1916 by Born[50], who treated the medium as an assembly of permanent electric dipoles and demonstrated the possibility of a transition from an isotropic phase to anisotropic one as the temperature is lowered. Though this result is important, qualitatively we need not discuss this particular theory because it is now well established that permanent dipole moments are not necessary for the occurrence of the liquid crystalline phase. Moreover, the theory predicts that the aligned phase should be ferroelectric, which does not appear to be

the case even when the molecules are polar. The most widely used treatment based on the molecular field approximation is that due to Maier and Saupe[51]. The theory assumes that (1) the molecules interact through an attractive orientation dependent van der Waals interaction (ii) the orientation dependent interaction does not affect the configuration of the centre of mass of the molecules and (iii) the molecules are assumed to be in an approximate mean field as described above. As a result a given molecule feels an effective potential of the mean field or single molecule potential or pseudopotential. This last assumption is not, however, quantitatively correct since intermolecular short range order and fluctuation effects are neglected.

In deriving the theory we shall follow the development of Humphries, James and Luckhurst[52]. We start with a completely general pairwise intermolecular interaction potential. After expanding in a series of appropriate spherical harmonics we will systematically average the pair-interaction potential to obtain a generalised version of the single molecule potential function in the mean field approximation. The Maier-Saupe theory will result from the retention of only the first term in the generalised potential. Many coordinates are required to describe the orientation dependent interaction between a pair of asymmetric molecules. Fig. 2.17(a) depicts the

situation. Since there appears to be no ordering of the molecules about their long axes the intermolecular pair potential V_{12} is a function of five coordinates[53].

$$V_{12} = V_{12}(r, \theta_1, \phi_1, \theta_2, \phi_2) \tag{2.2}$$

Pople[54], for axially symmetric molecules, expanded the pair potential as

$$V_{12} = 4\pi \sum_{L_1 L_2 m} U_{L_1 L_2 m}(r)\, Y_{L_1 m}(\theta_1, \phi_1)\, Y^*_{L_2 m}(\theta_2, \phi_2) \tag{2.3}$$

where $Y_{Lm}(\theta, \phi)$ are the usual harmonics. The expression is particularly convenient because it separates the distance and orientation dependence of the potential and the coefficients of the expansion, the $U_{L_1 L_2 m}(r)$ are found[55] to decrease rapidly with increasing L_1 and L_2. Further, terms only with even L_1 and L_2 are required since $\vec{n}$ and $-\vec{n}$ are equivalent.

In order to derive a mean field approximation to the potential V_{12} has to be expressed in terms of a polar coordinate system based on the director $\vec{n}$ as the polar axis. The coordinate axes of the molecules must be rotated from that shown in Fig. 2.17(a) to that shown in Fig. 2.17 (b). The primed angles now describe the orientation of the molecules with respect to the new rotated coordinate system. Mathematically this rotation

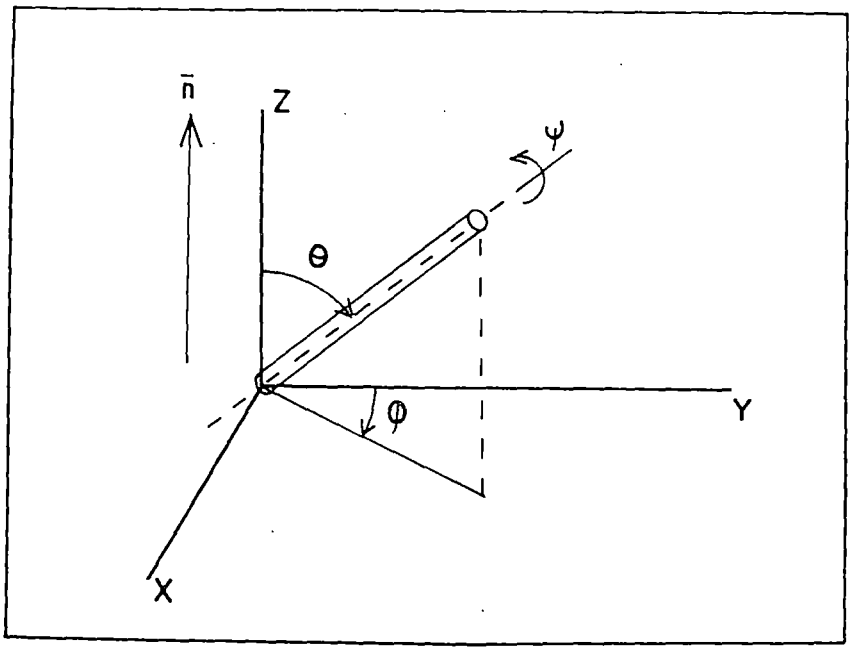

FIG. 2·16 The Euler angles required to describe the orientation of a molecule in nematic liquid.

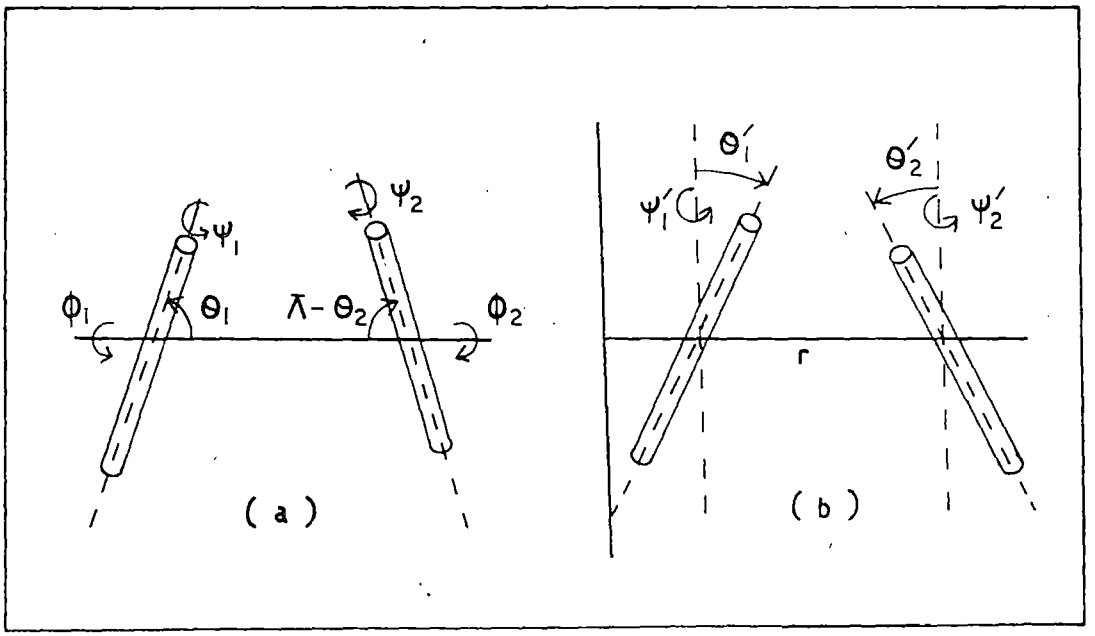

FIG. 2·17 The coordinate system required to describe the interaction between two asymmetric molecules: (a) the intermolecular vector is the mutual polar axis and (b) the director $\vec{n}$ is the polar axis for each molecule.

of the coordinate axes transforms the spherical harmonics into the form

$$Y_{Lm}(\theta,\phi) = \sum_{p} D_{pm}^{L}\, Y_{Lp}(\theta',\phi') \tag{2.4}$$

where D_{pm}^{L} are the elements of the Wigner rotation matrices[56]. Then

$$V_{12} = 4\pi \sum_{L_1 L_2 m} U_{L_1 L_2 m}(r)\, Y_{L_1 p}(\theta_1',\phi_1')\, Y_{L_2}^{*}(\theta_2',\phi_2') \cdot \left(D_{pm}^{L_1}\right)\left(D_{qm}^{L_2}\right)^{*} \tag{2.5}$$

From this pairwise intermolecular potential the pseudopotential can be obtained by taking three successive averages of V_{12}: (i) average over all orientations of the intermolecular vector $\vec{r}$ (ii) average over all orientations of the molecule 2, (iii) average over all values of $\vec{r}$. The results in[53]

$$\langle\langle\langle V_{12}\rangle\rangle\rangle = \sum_{Lm} \langle U_{LLm}(r)\rangle\, P_L(\cos\theta_1')\, \langle P_L\rangle \tag{2.6}$$

where P_L's are the Lth. order Legendre polynomials. This is the desired single-molecule potential in mean field approximation. We write it as

$$V_1(\cos\theta) = \sum_{L} U_L \langle P_L\rangle\, P_L(\cos\theta)$$

$$U_L = \sum_{m} \langle U_{LLm}(r)\rangle \tag{2.7}$$

Now it is mentioned earlier that L's should have only even values and since L = 0 is merely an additive constant eqn. (2.7) can be written as

$$V_1(\cos\theta) = U_2 \langle P_2 \rangle P_2(\cos\theta) + U_4 \langle P_4 \rangle P_4(\cos\theta) + U_6 \langle P_6 \rangle P_6(\cos\theta) + \cdots\cdots \tag{2.8}$$

Humphries et al[52] pointed out, if the true cylindrical symmetry of the distribution function for the orientation of the intermolecular vector were taken into account, terms proportional to

$$\langle U_{L_1 L_2 M}(r) \rangle (P_{L_1} \langle P_{L_2} \rangle + P_{L_2} \langle P_{L_1} \rangle) \tag{2.9}$$

would also appear in the single molecule potential V_1. If only the first term in eqn. (2.8) is retained we obtain the mean field theory of Maier and Saupe. Since the original expansion on which V_1 is based (eqn. 2.3) converges rapidly, retention of only the first term in V_1 should provide a good approximation to the theory. Comparison with experiment shows that this is indeed the case, addition of the higher order terms will of course result in a better agreement[57,58]. But negative values of $\langle P_4 \rangle$ found in some cases[58,59], cannot be predicted even if the higher order term is included in the mean field potential.

Now if $\rho(\cos\theta)$ designates the orientational distribution function which is the probability of finding a molecule at some prescribed angle θ from $\vec{n}$. then it can expressed in terms of V_1 as

$$\rho_1(\cos\theta) = Z^{-1} \exp\left[-\beta V_1(\cos\theta)\right]$$

$$\text{and} \quad Z = \int_0^1 \exp\left[-\beta V_1(\cos\theta)\right] d(\cos\theta)$$

(2.10)

where Z is the single molecule partition function, $\beta = 1/kT$, k being the Boltzmann's constant and T is the absolute temperature.

Since both V_1 and ρ_1 are even functions of $\cos\theta$ the integration is limited within 0 and 1. Eqn.(2.10) is not yet useful in computing average values since V_1 contains unknown averages $\langle P_L \rangle$

Now since $\langle P_L \rangle$ is the average value of Lth. order Legendre Polynomial we can write,

$$\langle P_L \rangle = \int_0^1 P_L(\cos\theta)\, \rho_1(\cos\theta)\, d(\cos\theta)$$

$$= \frac{\int_0^1 P_L(\cos\theta) \exp\left[-\beta V_1(\cos\theta)\right] d(\cos\theta)}{\int_0^1 \exp\left[-\beta V_1(\cos\theta)\right] d(\cos\theta)}$$

(2.11)

which is a self-consistent equation for the determination of the temperature dependence of $\langle P_L \rangle$. The simultaneous solution of equations (2.8) and (2.11), by using a computer, yields the temperature dependence of all the $\langle P_L \rangle$'s originally included in the potential V_1. In particular, the solution for $\langle P_2 \rangle$ gives the temperature dependence of the order parameter of the nematic phase.

Of all the possible solutions the one which satisfies the thermodynamic condition of minimum free energy will give the physically observed stable phase. For this we consider the Helmholtz free energy $F = E - TS$ where E is the internal energy and S the entropy though the Gibbs free energy should be considered in strict sense as most of the experimental measurements on order parameters are done under condition of constant pressure rather than at constant volume. For a system of N molecules we have expressions[53]

$$E = \tfrac{1}{2}N\langle V_1 \rangle = \tfrac{1}{2} N \sum_L U_L \langle P_L \rangle^2 \qquad (2.12)$$

$$S = -NK \langle \ln P_1 \rangle = N/T \sum_L U_L \langle P_L \rangle^2 + NK \ln Z \qquad (2.13)$$

$$F = -NK \ln Z - \tfrac{1}{2} N \sum_L U_L \langle P_L \rangle^2 \qquad (2.14)$$

The condition of minimum free energy i.e. $\left(\partial F / \partial \langle P_L \rangle\right)_{T,P_L} = 0$ regains the required self-consistency equation (2.11).

Rr

Furthermore testing eqns. (2.12) and (2.14) we see that they do satisfy the required thermodynamic identity $E = (\partial \beta F / \partial \beta)$. According to MS theory $\langle P_2 \rangle$ is a universal function of T/T_{NI}. But experimental values are found to differ slightly[60,61] from the predicted values. It may be noted here that U_2 which determines the strength of intermolecular potential depends on the molar volume V via intermolecular separation and this must change with temperature.

While elucidating the nature of intermolecular forces in nematics Maier and Saupe assumed that this was mainly due to London dispersion forces (i.e. induced dipole/induced dipole) which was dependent on the intermolecular separation as r^{-6} . So V_1 should depend on V^{-2}. Cotter[62] has shown that for the theory to have statistical mechanical consistency, the potential must have V^{-1} dependence rather than V^{-2} dependence of MS theory. So we shall be able to test the predictions of MS theory with the experimental values of $\langle P_2 \rangle$ at constant pressure.

While developing mean field theory Humphries et al[52] considered a volume dependence as $V^{-\gamma}$, γ being an adjustable parameter. Force fitting the experimental parameters, however, yielded values of γ as 10 in some cases[63] which are neither thermodynamically self consistent (V^{-1} dependence) nor consistent to dispersion

forces (V^{-2} dependence). Chandrasekhar and Madhusudan[57] obtained an volume dependence as V^{-3} considering permanent dipole-permanent dipole forces, induced dipole-induced quadrupole part of the dispersion forces. In view of these ambiguities regarding a knowledge of volume dependence, it is, however, preferable to treat the coefficients of V_1 in eqn. (2.8) as independent of volume and to restrict the fitting of the theory to experiment to a narrow range of temperature. Finally different forms of volume dependence may be included.

However, according to Luckhurst[64] the long wavelength orientational fluctuations in the medium diminish effective order parameter. The assumption that the molecule is a rigid rod is also an oversimplification and a realistic calculation has been made by Marcelja[65] taking the contribution of flexible and chain part in the ordering process which accounts for the alternation in the transition temperatures, the order parameter and other related properties of the successive members of a homologous series. Recent theoretical work by Luckhurst[66], however, shows the effect of the flexibility of molecules on order parameter is only marginal.

Order parameters of different mesophases (specially for nematics) have been determine by many workers employing various experimental techniques viz. diamagnetic anisotropy[67], optical anisotropy[67,68], magnetic resonance spectroscopy[69], Raman scattering[70,71], infrared spectros-

copy[71], UV and visible spectroscopy[70], Mössbauer spectroscopy[72], neutron scattering[72], positron anhilation[72], dielectric axm anisotropy[72], Guest-host interaction[73,74], X-ray diffraction etc. Comparison of these results with Maier-Saupe theory has briefly been discussed by Smith[75]. The details of all the experimental techniques are reviewed by different workers[72]. In this dissertation we shall discuss in subsequent section only the X-ray diffraction technique.

2.5. Theoretical background for X-ray diffraction work:

From X-ray diffraction study we can get idea about molecular interactions in liquid crystals. First attempt was made by Lingen and Friedel[76,77], immediately after the discovery of X-ray diffraction. Lots of studies made in this area have been reviewed in references[78-81] and the detail theoretical considerations are given by Vainshtein[82] and Luckhurst[83]. Generally, nematic liquid crystal samples consist of a large number of domains, the molecules being ordered within each domain along the director $\vec{n}$, but there is no preferred direction for the specimen as a whole. So the X-ray diffraction pattern has a symmetry of revolution around the direction of the X-ray beam as is evident from the uniform halo just like that of an isotropic liquid. Diffraction photographs of the specimen oriented by some means are, therefore, needed to specify the state of ordering. For samples oriented perpendicular to the

incident X-ray the diffuse main ring (halo) splits into two crescents symmetrical about the origin. The halo or the crescents appear due to intermolecular scattering. The intensity maxima of the crescents lie in the equatorial section i.e. perpendicular to the optic axis (director). Some other rings are also observed in the meridional section (parallel to the director) which are due to intramolecular scattering. From the distribution of intensity in the equatorial plane of the diffraction pattern (of oriented sample), one can obtain the atomic cylindrical distribution function, giving the probability of finding two atoms at a particular distance, the atoms may, however, belong to same or different molecules. Moreover, according to Chistyakov[80], the method involves an integration over the scattering vector from zero to infinity which can never be fulfilled by photographic methods with a flat plate camera, the plate being normal to the X-ray beam. Calculation of cylindrical distribution function and order parameters from X-ray diffraction works has later been done by de Vries[84] while orientational distribution function and order parameters have been calculated by various workers[85-90].

2.3.1. Orientational distribution functions and order parameters:

The average state of orientation for a system of cylindrically symmetric molecules can be sufficiently described by a distribution function $f(\beta)$ depending only on the angle between the molecular symmetry axis and the director[88] as mentioned in section 2.2.3. X-ray diffraction photographs record intensities averaged over a relatively long time and over a macroscopic volume, so the molecules may be assumed to have an average cylindrical symmetry even if they do not rotate about their long axes[87]. The order parameters $\langle P_L \rangle$ for a system of rigid rods in a uniaxial phase are therefore, defined as,

$$\langle P_L \rangle = \frac{\int_0^{\pi/2} P_L(\cos\beta) \cdot f(\beta) \cdot \sin\beta \, d\beta}{\int_0^{\pi/2} f(\beta) \sin\beta \, d\beta} \qquad (2.15)$$

with $L = 2$ and 4. In relating the X-ray intensity $I(\psi)$ around the diffuse equatorial arc (Fig. 2.18) with the orientational distribution function $f(\beta)$, Leadbetter and Norris[87] assumed that the rigid rod like molecules are perfectly aligned in a cluster of a small number of molecules ($\gtrsim$ 10) and obtained

$$I(\psi) = c \int_{\beta=\psi}^{\pi/2} f_d(\beta) \sec^2\psi \left[\tan^2\beta - \tan^2\psi\right]^{-1/2} \sin\beta \, d\beta \qquad (2.16)$$

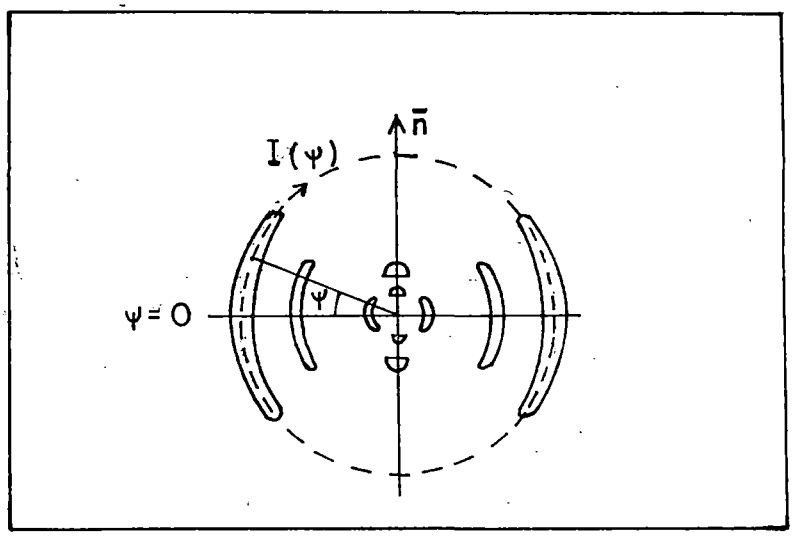

Fig. 2.18 Schematic representation of the X-ray diffraction photograph of an oriented liquid crystal.

where $f_d(\beta)$ now describes the distribution function of the clusters in which the molecules are perfectly aligned rather than the true singlet distribution function $f(\beta)$. They have also assumed that for a perfectly aligned sample $[f_d(\beta) = \delta(\beta)]$ the scattering is zero except for the directions of the scattering vector perpendicular to cluster axis. They have however, calculated the effects and found that the deviation is small except for highly ordered phases ($\langle P_2 \rangle \geq 0.8$). Moreover, comparing the values of $f_d(\beta)$ with $f(\beta)$ of the same sample obtained by other methods they showed that $f_d(\beta)$ may well be replaced by $f(\beta)$ values.

The method of obtaining intensity values $I(\psi)$ from the measured optical densities of the X-ray diffraction photographs will be described in sections 2.4.1 and 2.4.3. For evaluating the integrals in eqn.(2.15) and 2.16 angular scanning for one quadrant ($\psi = 0$ to $\psi = \pi/2$) is sufficient. We have, however, calculated $f(\beta)$ and order parameters values for each of the quadrants separately and then took the average. At the same time we used the mean $I(\psi)$ values of the four quadrants to obtain $f(\beta)$, $\langle P_2 \rangle$ and $\langle P_4 \rangle$ values. Two sets of values being almost equal we have calculated them using mean $I(\psi)$ values.

The molecular orientational distribution function and intensity distribution function can be expanded as a power series only with even terms[87,90]. Therefore, we write

$$I(\psi) = \sum_{n=0}^{r} a_{2n} \cos^{2n} \psi \qquad (2.17)$$

$$f(\beta) = \sum_{n=0}^{r} b_{2n} \cos^{2n} \beta \qquad (2.18)$$

Eqn. (2.16) is modified, by substituting $\sin\alpha = \cos\beta \sec\psi$, to

$$I(\psi) = c \int_{0}^{\pi/2} f_1(\alpha) \sin\alpha \, d\alpha \qquad (2.19)$$

From eqns. (2.17), (2.18) and (2.19), therefore, have

$$\sum_{n=0}^{r} a_{2n} \cos^{2n} \psi = \int_{0}^{\pi/2} \sum_{n=0}^{r} b_{2n} \cos^{2n} \psi \sin^{2n+1} \alpha \, d\alpha$$

$$= \sum_{n=0}^{r} b_{2n} \cos^{2n} \psi \int_{0}^{\pi/2} \sin^{2n+1} \alpha \, d\alpha \qquad (2.20)$$

Since ψ is arbitrary, the coefficients of $\cos^{2n} \psi$ must be equal.

Now

$$\int_0^{\pi/2} \sin^{2n+1}\alpha \, d\alpha = \frac{2^{2n}\,(n!)^2}{(2n+1)!}$$

and so

$$b_{2n} = a_{2n} \cdot \frac{(2n+1)!}{2^{2n}\,(n!)^2} \qquad (2.21)$$

The series in Eqns. (2.17) and (2.18) converge rapidly. Retaining eight terms in the truncated series, a least squares fitting was made to obtain the coefficients from Eqn. (2.17) with corrected experimental intensity values. The calculated intensities in all cases were found in good agreement with the observed intensities. These values of a_{2n} were then used to calculate the coefficients b_{2n}. Then $f(\beta)$ values were calculated using the eight term series.

By calculating the integral

$$\int_0^{\pi/2} f(\beta) \sin\beta \, d\beta = K \text{ (say)},$$

and then dividing all the b_{2n} values by K we obtained the normalized values of the orientational distribution function. Substituting Eqn. (2.18) in eqn. (2.15) we

get

$$\langle P_2 \rangle = \frac{1}{2} \frac{\int_0^1 (3\cos^2\beta - 1) \sum_{n=0}^{n} b_{2n} \cos^{2n}\beta \, d(\cos\beta)}{\int_0^1 \sum_{n=0}^{n} b_{2n} \cos^{2n}\beta \, d(\cos\beta)}$$

(2.22)

This can be written in terms of the standard integrals and $\langle P_2 \rangle$ can be calculated and similarly $\langle P_4 \rangle$

From the uncertainties in the measurement of optical densities and corresponding intensity values the errors in $\langle P_2 \rangle$ and $\langle P_4 \rangle$ values were estimated by drawing different intensity distribution curves within the range of uncertainty. For all these curves $\langle P_2 \rangle$ and $\langle P_4 \rangle$ were calculated and accuracy of both the parameters were always found to be better than $\pm$ 0.02. It is to be noted, however, that uncertainty in the temperature, background correction and irregularity in the film coating (if any) could not have been taken into account in the error estimation.

2.3.2. Pseudopotential:

The normalised distribution function can be written as (section 2.2)

$$f(\beta) = Z^{-1} \exp\left[-V(\beta)/kT\right] \tag{2.23}$$

where Z is the orientational partition function which at a particular temperature was treated as constant and $V(\beta)$ is the angular part of the intermolecular potential. We have fitted our $f(\beta)$ values to the form

$$f(\beta) = Z^{-1} \exp\left[\sum_{L\,\text{even}} c_L P_L(\cos\beta)\right] \tag{2.24}$$

or

$$\ln f(\beta) = \sum_{L\,\text{even}} c_L P_L(\cos\beta) + \text{constant} \tag{2.25}$$

A least square fitting of Eqn. (2.25) with calculated $f(\beta)$ values for different β at a particular temperature gives c_L. In this fitting six terms are retained in the series to obtain a good idea about the pseudopotential. Bhattacharjee et al.[91] in our laboratory earlier analysed the errors in calculating the coefficients c_L ($\equiv c_0 \equiv -\ln Z$) and found the first few (upto $L = 4$) coefficients to be well defined within an accepted range of values.

A general anisotropic pair potential may be constructed (sec. 2.2) as

$$V(\beta) = \sum_{L\,\text{even}} d_L \langle P_L \rangle P_L(\cos\beta) \qquad (2.26)$$

where the coefficients d_L can now be obtained comparing Eqns. (2.24) and (2.26) as

$$d_L = - \frac{c_L kT}{\langle P_L \rangle} \qquad (2.27)$$

We have calculated d_2 and d_4 for different temperatures. Since the coefficients d_L determines the strength of the intermolecular forces, they should depend on the intermolecular separation and so on temperature. Initially we treated (as discussed earlier) d_L as constants independent of temperature and constructed the pseudopotential taking the average values of d_2 and d_4 for different temperatures and then included density dependence. With this pseudopotential thus constructed the normalised N distribution function $f(\beta)$ values were calculated both retaining $\langle P_2 \rangle$ and $\langle P_4 \rangle$ terms using Eqn.(2.23). In this calculations, Z was adjusted so that $f(\beta)$ values were normalised. These normalised distribution function values were then compared with the experimental $f(\beta)$ values.

According to Vainshtein[62] a fairly good approximation for order parameters can be obtained by replacing $f(\beta)$ values with $I(\psi)$ values (at a constant Bragg angle). We have also calculated order parameters using this approximation and designated them as $\langle P_2 \rangle_v$ and $\langle P_4 \rangle_v$

2.3.3. Molecular parameters :

From the diffraction ring diameter one obtains the corresponding diffraction angle 2θ. The spacing X between two successive reflecting points or planes is related to the corresponding diffraction angle by a formula of the type[92],

$$2X \sin\theta = K\lambda \qquad (2.28)$$

where λ is the wavelength of the X-ray and K is a constant depending on the shape and arrangement of the molecules[93]. Our experiments concern with two spacings giving two diffraction maxima positions at widely different angles. That the outermost appears due to interaction of neighbouring parallel molecules while the inner ring is in some way related to the length of the molecule, was established by de Vries[9, 94]. They also discussed in detail the choice of K in eqn. (2.28) depending on particular spacing we are concerned with as well as the shape and orientation of the molecules. We used K = 1 for inner maxima i.e. Bragg law.

For outer maxima, we however, used K = 1.117 for both oriented and unoriented samples. This is because if we consider the scattering from a pair of molecules at a distance D apart and if the chains are allowed to rotate x freely around each other, the positions of the maxima along the equator are determined by the function[9]

$$J_0(x) = \int_0^{2\pi} \cos(x \cos\alpha)\, d\alpha$$

where $x = 4\pi/\lambda \cdot d \cdot \sin\theta$ and this gives for first maxima K = 1.117.

Wendorff et al[92] calculated K values from the photograph of some cholesterol esters by taking X values in eqn. (2.28) from completely extended form of the molecule and found that K lies between 1 for perfectly ordered molecules and 1.229 for completely random orientation of the molecules.

2.4. Experimental Techniques and data analysis:

All the X-ray diffraction photographs were taken in flat plate camera with Radon House (India) X-ray generator. An X-ray tube with Cu-target was used. The flat plate camera used for taking X-ray photographs was m equipped with high temperature arrangement fabricated by Jha and Paul[95] in our laboratory. This set up also has provisions for interchangable collimator, interchangable spacer to vary the sample to film distance and interchangable pole pieces gap of the electromagnet. Fig. 2.19 shows the sectional diagram of the whole arrangement.

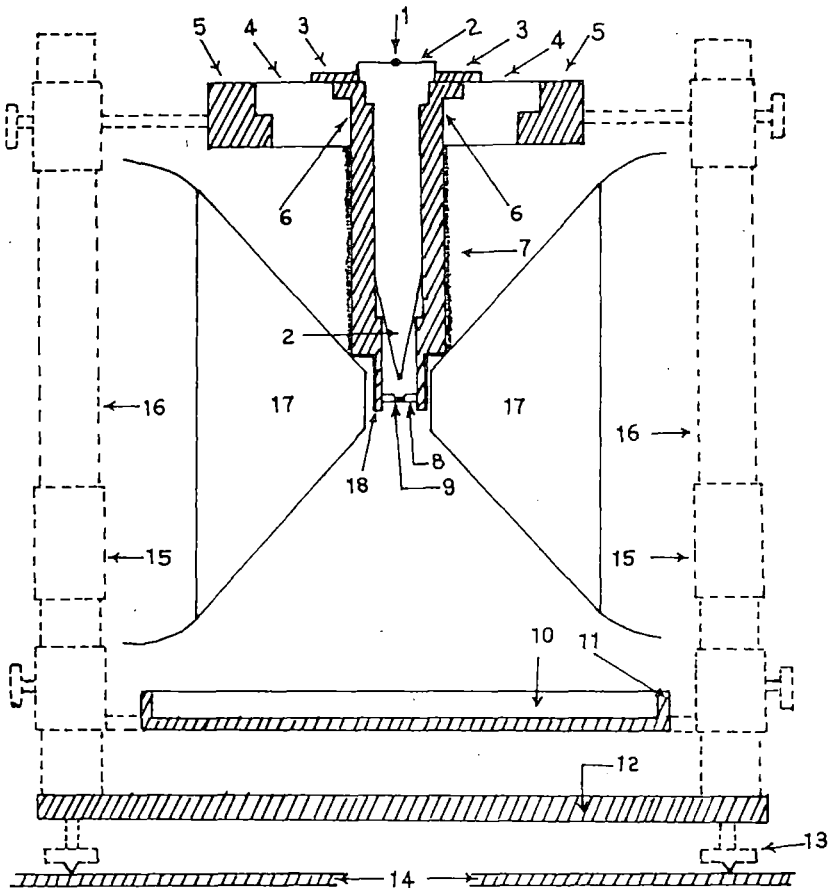

Fig.2.19.Sectional diagram of the camera:
(1) X-Ray; (2) Collimator; (3) Brass Ring; (4) Ring of Syndanio Board; (5) Brass Ring; (6) Cylindrical Brass Chamber; (7) Asbestos Insulation and Heater Winding; (8) Specimen Holder and Thermocouple; (9) Specimen; (10) Film Cassette; (11) Film Cassette Holder; (12) Base Plate; (13) Levelling Screw; (14) Brass Plates over the Coils of Electromagnet; (15) Removable Spacer; (16) Supporting Brass Stands; (17) Polepieces; (18) Asbestos insulation.

All the materials used are non-magnetic. A vertical X-ray beam incidents on the specimen (9) through the collimator (2) which is push fit into the sample holder. The cylindrical brass chamber (6) has heating coils wx which are insulated by asbestos fibre (7). The sample holder (8) is well insulated by asbestos sheets and sindanyo boards(4) from the posts (16) supporting the sample holder (8), the sample being taken in a thin walled gm glass capillary of diameter 1.0 mm. approximately. The sample holder including the insulation can be reduced to 1.0 to 1.5 cm. thickness at the position of the sample so that a strong magnetic field can be applied. The four supporting posts are rigidly attached to a heavy brass plate (12). The film cassette is mounted on a cassette holder (11) which is also supported by the posts. Spacer (15) can be introduced along the posts between the clamps of the cassette holder and the sample holder and also between the cassette holder and the heavy brass plate so that reproducible geometry can be obtained. Levelling screws (13) can be used for adjustment and better collimation. The pole pieces (17) of the electromagnet can be brought very close to the sample holder, the pole pieces were properly shaped for this purpose for production of strongest field at the specimen position.

The X-ray tube is enclosed in an iron container in order to provide magnetic sheilding to high speed electrons and in order to avoid the attraction of the

tube by the magnet it is supported by a wooden block placed over the pole pieces. The temperature was regulated within $\pm$ .5°C by supplying variable voltages to the heating coils from a stabilized power supply and was measured with the help of a sensitive galvanometer and lamp-scale arrangement and calibrated copper-constantan thermocouple. The sample holder was calibrated upto 250°C with a number of samples of known melting points.

The strength of the magnetic field at a fixed distance (2.0 cm.) was measured for different currents by a sensitive galvanometer (ECIL model GM867). For all photographs Cuk$_\alpha$ radiation monochromated by a Ni-filter of thickness .009 mm. was used, the beam was being collimated by a collimator of aperture 0.8 mm. While taking unaligned photographs by this set up the pole pieces were removed. To have better resoluted low angle diffraction pattern from a unaligned sample a Universal Camera (URK 3, VEB FREIBERGER PRAZISIONSMECHANIK, GDR) with high temperature attachement developed by us was also used in some cases.

For each observation set, the exact distance between the sample and the film was determined by taking Al-powder photograph. Since for Al the unit cell dimension is known, the Bragg angle for hkl reflecting plane can be determined from[96]

$$\sin\theta = \lambda/2a \sqrt{h^2 + k^2 + l^2} \qquad (2.29)$$

Thus knowing Bragg angles corresponding to 111 and 200 observed diffraction rings[97] and measuring their diameter from the photograph the exact sample to film distance can be obtained from the relation

$$\tan 2\theta = \frac{\text{Radius of the ring}}{\text{Sample to film distance}} \qquad (2.30)$$

Then a correction term is calculated and applied to the spacer separation to obtain the exact distance.

2.4.1. Conversion of optical density to X-ray intensity:

In order to determine various parameters, the X-ray diffraction photographs were scanned both linearly and circularly with a Carl Zeiss Microdensitometer (MD 100) which has potentiometric recording (K 200) facility for linear scanning. The circular scanning was made manually, the rotation stage was modified by us for this purpose. The optical densities obtained from densitometric scanning were then converted to relative intensities by a method adopted by Klug and Alexander[98]. An intensity scale was prepared by exposing different portion of a film to X-rays coming through a small rectangular opening with exposure times 5, 10, 15, 20 .....secs. Multiple film technique was used. Optical densities of these spots were then measured with the microdensitometer and a graph was drawn by plotting optical density versus time in secs. (i.e. X-ray

intensity). This is shown in Fig. 2.20. While measuring the optical densities of X-ray diffraction photograph and gradiation strip, the densitometer zeroing was made on unexposed X-ray films, no subtraction for unexposed film optical density was, therefore, necessary. However, the brand and type of the film, the developing time, composition and temperature of the developer have pronounced effect upon both the optical density and film factor of the response curve. So these quantities were tried to keep to the same values as applied to prepare gradiation strip.

2.4.2. Linear scanning and location of peak positions :

We mentioned earlier that in order to calculate the average intermolecular distance (D), the diameter of the outer diffraction maxima (ring, halo or crescents) is to be determined. From the linear scanning of the outer maxima through the central spot using the potentiometric recorder a graph relating optical density vs. linear distance as shown in Fig. 2.21 is obtained. The difference between the peak points of the outer maxima gives its diameter. There are different methods[99] for locating the peak position from linear distance vs. O. D. curve as shown in Fig.2.22. P_o is the apparent maximum of the line profile. It had the drawback that statistical uncertainity in the optical density values at and in the immediate vicinity of the maximum makes its precise location uncertain. In order to

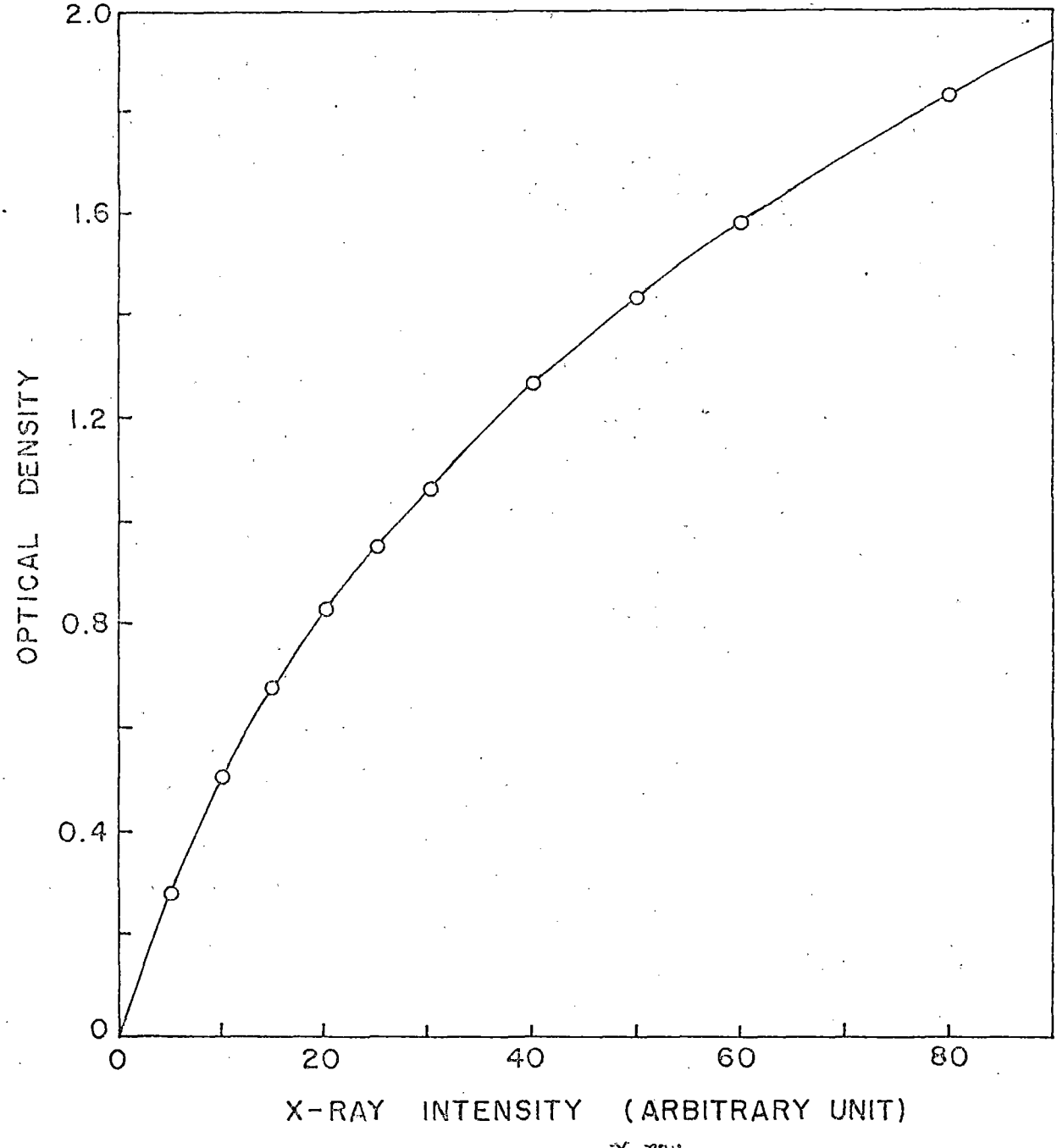

Fig. 2.20 Optical density vs. X-ray intensity curve.

avoid this problem a commonly employed method is to locate the peak at P_x, the point of intersection of two straight lines projected from the most linear portions of the sloping sides of the profile. Another method is to assign the peak position to the mid point of a chord drawn parallel to the background and located at one half of the maximum peak optical density $P_{1/2}$ or better at higher levels such as $P_{2/3}$ or $P_{3/4}$. The different methods give some what different values for the peak position despite the relative sharpness of the line profiles. When the peak is well defined we, however, simply take the P_o position, in other cases we used $P_{2/3}$ position. Knowing the diameter, the Bragg angle θ corresponding to this diffraction ring is determined using Eqn. (2.30) when the actual sample to film distance is known, and then the average intermolecular distance (D) is calculated using eqn. (2.28). The same procedure is adopted to determine the diameter of the inner ring.

In order to get the diameter of the outer crescents accurately, the linear scanning was made on different asimuthal angular positions. Considering $\Psi = 0$ at the maximum intensity position, the linear scanning is done for $\Psi = 0, \pm 30^{0}$. The mean of the diameters obtained was taken as the actual diameter.

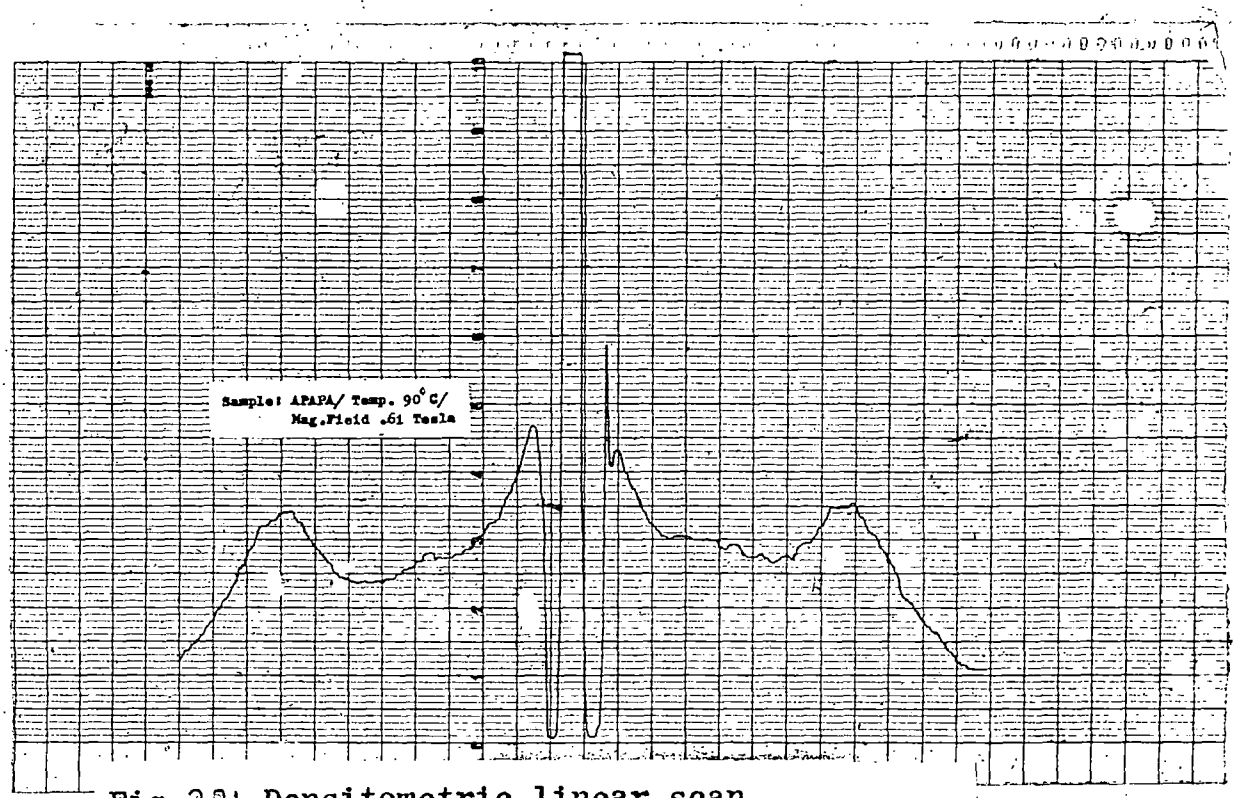

Fig.2.21 Densitometric linear scan.
Scanned through outer maxima points.

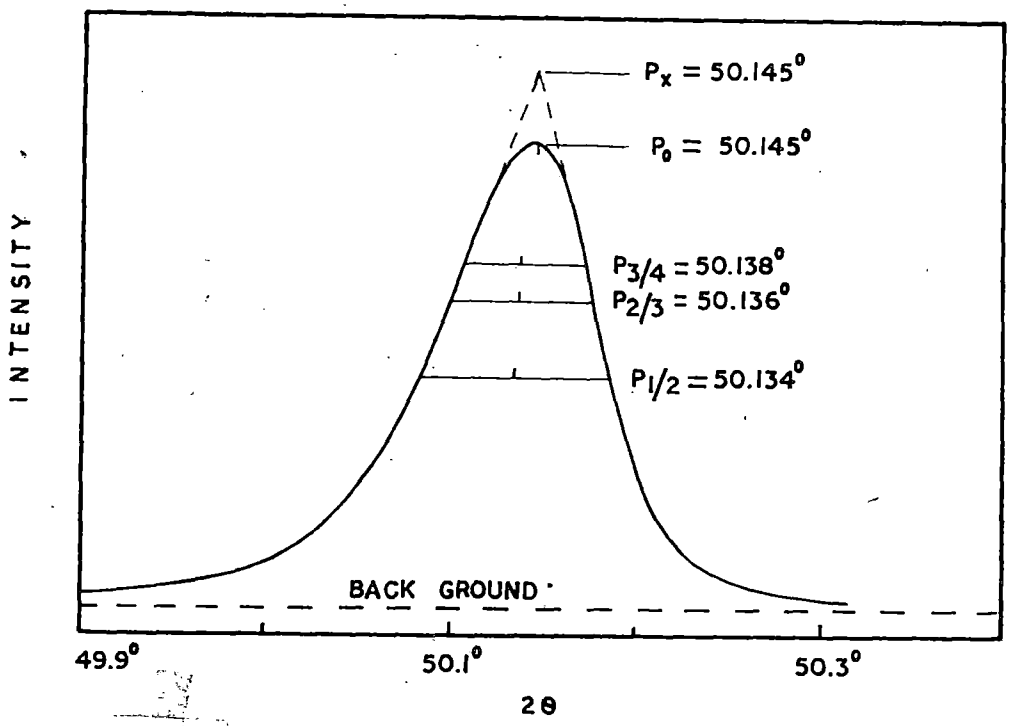

FIG. 2.22 VARIOUS METHODS OF LOCATING THE PEAK POSITION OF A LINE PROFILE.

2.4.3. Circular scanning and to plot I (ψ) versus ψ curve:

In order to determine the orientational distribution function $f(\rho)$, order parameters $\langle P_2 \rangle$ and $\langle P_4 \rangle$ circular scanning of the outer diffraction ring as shown in Fig. 2.18, is required. The values of optical densities obtained from the densitometric circular scanning are converted to X-ray intensities with the help of callibration curve. The converted intensities are then plotted against different azimuthal angular positions. The intensities are corrected from the background intensity values arising due to air scattering. This is accomplished by drawing tangents through the minimum of the intensity distribution curve and then subtracting the values on the tangent from the corresponding observed intensity values. The peak intensity position which would correspond to $\psi = 0$ was determined at the position where the height of the angle vs. intensity curve above the background line was maximum (Fig. 3.8). However, in some cases, some unwanted spots or even a slight nonuniformity in film coating raised some problems. So a smooth curve was drawn through a large number of points and in determing the peak positions care was taken, where such ambiguites arose, to see that I (ψ) was more or less symmetric around $\psi = 0$. We have used the mean I (ψ) values of the four quadrants to obtain $f(\rho)$, $\langle P_2 \rangle$ and $\langle P_4 \rangle$ values.

Taking nineteen I (ψ) values from $\psi = 0^0$ to $\psi = 90^0$ at five degrees interval from I (ψ) vs. ψ curve $f(\beta)$ and $\langle P_L \rangle$ were calculated using Leadbetter's approximation. Then $f(\beta)$ vs. β curve was drawn. A computer programme was developed for this calculation to use in Wipro Series 8600 computer system.

References

1. H.Sackmann and D.Demus, Mol.Cryst.Liq.Cryst., 21, 239 (1973).
2. A. de Vries, Pramana Suppl.No.1, 93 (1975).
3a. A. de Vries, Liquid Crystals, The Fourth State of Matter, ed.F.D.Saeva, Marcell Dekker, Inc, NY, p.1 (1972).
b. A. de Vries, Mol.Cryst.Liq.Cryst., 63, 215 (1981).
4. S.E.B. Petrie, Ref.3a, p. 163.
5. J. Doucet, The Molecular Phys. of Liquid Crystals, Eds. G.R.Luckhurst and G.W.Gray, Academic Press, NY, p. 285 (1979).
6. L.V.Azaroff, Mol.Cryst.Liq.Cryst., 60, 73 (1980).
7. D.Demus, J.W.Goodby, G.W.Gray and H. Sackmann, Mol. Cryst. Liq.Cryst., 56, 311 (1980).
8a. G.W.Gray, Ibid, 67, 3 (1981).
b. J.W.Goodby and G.W.Gray, Ibid, 41, 145 (1978).
9. A. de Vries, Mol.Cryst.Liq.Cryst. 10, 31 & 219 (1970).
10. P.G. de Gennes, The Phys. of Liquid Crystals, Clarendon Press, Oxford, p.7 (1974).
11. G.G.Fryberg, E.Golerinter and D.L.Fichel, Mol.Cryst. Liq.Cryst., 16, 39 (1972).
12. S.Diole, F. Brand and H.Sackmann, Ibid, 16, 105 (1972)
13. G.R.Luckhurst and A.Sauson, Ibid, 16, 179 (1972).
14. A. de Vries, Mol.Cryst.Liq.Cryst. 49 (Lett), 143 (1979).
15. A. de Vries, A. Ekachi and N.Spielberg, Ibid, 49, 143 (1979).

16. N.H.Tinh, P.Foucher, C. Destrade, A.M.Levelut and J.Malthete, Mol.Cryst.Liq.Cryst., 111, 277 (1984).

17. S.Diele, G.Pelzl, I.Latif and D.Demus, Ibid, 92, 27 (1983).

18. N.A.P. Vaz., Z.Yaniv and J.W.Doane, Ibid, ~~Lett~~, 92, 75 (1983).

19. P.E.Cladis, Phys. Rev.Letts., 35, 48 (1977) P.E.Cladis, R.K.Bogardus,W.B.Daniels and G.N.Taylor,Ibid, 39, 720 (1977).

20. F.Hardouin, A.M.Levelut, J.Bennattar and G.Sigaud, Solid.State.Comun., 33, 337 (1980).

21. F.Hardouin and A.M.Levelut, J.Phys.(Paris), 41, 41 (1980).

22. G.Sigaud, N.A. Tinh, F.Hardouin and H.Gasparoux, Mol.Cryst.Liq.Cryst., 69, 81 (1981).

23. B.V.Madhusudana, B.K.Sadashiva and K.P.L.Moodithya, Curr.Sci.48, 613 (1979).

24. F.Hardouin, G.Sigaud, M.F.Achard and H.Gasparoux, Phys. Lett., 71A, 347 (1979).

25. G.J.Brownsey and A.J.Leadbetter, Phys.Rev.Lett., 44, 1608 (1980).

26. A.J.Leadbetter, J.C.Frost,J.P.Gaughan, G.W.Gray and A.Mosley, J.Phys.(Paris), 40, 375 (1979).

27. K.A.Suresh, R.~~Xxx~~ Nashidhara, G.Heppke and R.Hopf, Mol.Cryst.Liq.Cryst.99, 249 (1983).

28. A. de Vries, J.Phys. (Paris), Colloq.,36, C1-1(1975).

29. S.Diele, P.Brand and H.Sackmann, Mol.Cryst. Liq. Cryst., 17, 163 (1972).

30. G.W.Gray and P.A.Winsor, Ibid, 26, 305 (1974).

31. A.J.Leadbetter,J.P.Gaughan, B.Kelly, G.W.Gray and J.W.Goodby, J.Phys. (Paris), 40, 178 (1979).

32. S.Miele, D.Demus and H.Sackmann, Mol.Cryst.Liq. Cryst. 56 (Lett), 217 (1980).

33. P.A.C.Gane, A.J.Leadbetter and P.G. Wrighton, Mol.Cryst.Liq.Cryst., 66, 247 (1981).

34. R.J. ~~Xxx~~ Birgeneau and J.D. Litster, J. Phys. (Paris), Letts. 39, L-399 (1978).

35. R.M.Richardson, A.J.Leadbetter and J.C.Frost, Ann.Phys. 3, 177 (1978).

36. A .J.Leadbetter, M.A.Mazid and R.M.Richardson, Liquid Crystals, Ed.S.Chandrasekhar, Heyden, London, p.65 (1980).

37. A.J.Leadbetter,M.A.Mazid, B.A.Kelly,J.W.Goodby and G.W.Gray, Phys.Rev.Lett., 43, 630 (1979).

38. J.Doucet, A.M.Levelut, M.Lambert, L.Liebert and L.Strzelecki, J. Phys. (Paris), Colloq.36: C1-13 (1975).

39. D.Coates, G.W.Gray and K.J.Harrison, Mol.Cryst. Liq.Cryst., 22, 99 (1973).

40. A. de Vries, Mol.Cryst.Liq.Cryst. 24, 337 (1973).

41. A. de Vries, and D.L.Fishel, Ibid, 16, 311 (1972).

42. D.B.Chung, Ph.D.Dissertation, Kent State Univ., Kent, Ohio, p.75 (1974).

43. A.J.Leadbetter and R.M.Richardson, The Mol.Phys. of Liquid Crystals, Eds. G.R.Luckhurst and G.W.Gray, Academic Press, London, p.451 (1979).

44. A.J.Dianoux and F.Volino, J.Phys. (Paris), 40, 181 (1979).

45. J.Doucet, P.Keller, A.M.Levelut and P.Porquet, J. Phys. (Paris), 36, 548 (1978).

46. R.B.Detjen, D.L.Uhrich and G.F.Sheley, Phys. Letts. 42A, 522 (1973).

47a. J.R.Flick, A.S.Marshall and S.E.B.Petrie, Liquid Crystals and Ordered Fluids, Eds. J.F.Johnson and R.S.Porter, Plenum Publishers,NY,Vol2,p.97 (1974).

b. S.L.Arora, T.R.Taylor and J.L.Fergason, Ibid,Vol.1, p.321 (1970).

c. R.D.Ennulat, Mol.Cryst.Liq.Cryst.3, 405 (1967).

48a. R.Williams, J.Chem. Phys.50, 1324 (1969).

b. D.Mayerhofer, A.Sussman and R.Williams, J.Appl. Phys. 43, # 3685 (1972).

49. J.W.Emsley, S.K.Khoo and G.R.Luckhurst, Mol.# Phys. 37, 959 (1979).

50. M.Born, Sitz. d. Phys. Math., 25, 614 ~~(1961~~ (1916).

51. W.Maier and A.Saupe, Z.Naturforsch, 13a, 564 (1958); 14a, 882 (1959); 15a, 287 (1960).

52. R.L.Humphries, P.G.James and G.R.Luckhurst, J.Chem. Soc. Farad.Trans.II, 68, 1031 (1972)

53. Ref.8, p.46.

54. J.A.Pople, Proc.Roy.Soc. A221, 498 (1954).

55. J.R.Sweet and W.A.Steele, J.Chem.Phys., 47, 3022(1967)

56. M.E.Rose, Elementary Theory of Angular Momentum, J.Willey and Sons, NY (1957).

57. S.Chandrasekhar and V.N.Madhusudana, Acta Cryst, A27, 303 (1971)

58. S.Jen, N.A.Clark, P.S.Pershan and E.B.Priestley, Phys. Rev. Lett. 31, 1552 (1973).

59. S.Kobinata, Y.Nakajima, H.Yoshida and S.Maeda, Mol.Cryst.Liq.Cryst.66, 287 (1981).
Phys. Soc.Japan, 49, 1140 (1980).

60. A. Saupe, Angew Chemie, 7, 97 (1968).

61. S.Chandrasekhar and N.V.Madhusudana, J.Phys.(Paris), 30, 24 (1969).

62. M.A.Cotter, Mol.Cryst.Liq.Cryst.39, 173 (1977).

63. G.R.Luckhurst, The Mol.& Phys. of Liquid Crystals, Eds. G.R.Luckhurst and G.W.Gray, Academic Press, Ch. IV (1979).

64. G.R.Luckhurst, Quant.Rev. 22, 179 (1968), Mol.Cryst. Liq.Cryst., 21, 125 (1975).

65. S. Marcelja, J.Chem.Phys. 60, 3599 (1974).

66. G.R.Luckhurst, Mol.Cryst.Liq.Cryst., 72 (Lett) 201 (1980).

67. A.Saupe and W.Maier, Z.Naturforsch, 16a, 816 (1961).

68a. P.Chatelian, Bull.Soc.France,Miner.Cryst.78, 262 (1955).

b. Ref. 61.

c. S.Chandrasekhar,Mol.Cryst.Liq.Cryst. 16, 21 (1972).

69. P.L.Nordio and U.Segre, The Mol.& Phys. of Liquid Crystals, Eds. G.R.Luckhurst and G.W.Gray, Academic Press (1979).

70. P.S.Pershan, Ibid, p. 384(1979).

~~71. V.V.Rao, Liquid Crystals and Plastic Crystals, Eds. G.W.Gray and P.A.Winsor, Ellis Horwood and Sons,~~

71. V.V.Neff, Liquid Crystals and Plastic Crystals, Eds. G.W.Gray and P.A.Winsor, J.Willey and Sons, INC, Vol.II (1974).

72. H. Kelkar and R.Hatz, Handbook of Liquid Crystals, Verlag Chemie, Ch.5 (1980).

73. G.H.Heilmier and L.A.Zanoni, Appl. Phys. Lett., 91 (1968).

74. R.J. Cox, Mol.Cryst.Liq.Cryst., 55, 1 (1979).

75. G.W.Smith, Advances in Liquid Crystals Vol.I, Ed.G.H.Rx Brown, Academic Press (1975).

76. J.S.V.D. Lingen, Ber.Dt.Chem.Ges., 15, 913 (1913).

77. G.Friedel, Annls.Phys. 18, 273 (1922).

78. J.Falgueirettes and P.Delord, Liquid Crystals and Plastic Crystals, Eds. G.W.Gray and P.A.Winsor, Ellis Horwood, Vol2, Ch.3 (1974).

79. Ref. 72, Ch.5 (1980).

79a. G.H.Brown and W.G.Shaw, Chem.Rev., 57, 1049 (1957).

79b. G.W.Gray, Molecular structure and the properties of Liquid Crystals, Academic Press, London & NY(1962)

80. I.G.Chistyakov, Sov.Phys.Usp., 9, 551 (1967).

81. L.V.Azaroff, Mol.Cryst. Liq.Cryst., 60, 73 (1980).

82. B.K.Vainshtein, Diffraction of X-rays by Chain Molecules, Elsevier, Pub.Co. (1966).

83. Ref. 63, ch.13.

84. A.de Vries, J.Chem. Phys. 56, 4489 (1972).

85. P.Delord and J.Falgueirettes, Cr.hebd. Seanc. Acad.Sci.Paris, 260, 2468 (1965).

86. J.Felgueirettes, Bull.Soc.fr.Miner Crystallography, 82, 171 (1959).

87. A.J.Leadbetter and M.K.Norris, Mol.Phys., 38, 669 (1979).

88. C.Zannoni, The Mol.Phys. of Liquid Crystals, Eds. G.R.Luckhurst and G.W.Gray, Acadamic Press, Ch.5 (1979).

89. A.J.Leadbetter and P.G.Wrighton, J.Phys.(Paris), Collq., 40c, 3 (1979).

90. Ref. 10, ch.2

91. B.Bhattacharjee, S.Paul and R.Paul, Mol.Phys. 44, 1391 (1981).

92. J.H.Wendorff and P.P.Price, Mol.Cryst. Liq.Cryst. 24, 129 (1973).

93. I.G.Chistyakov, R.I.Schabischev, R.I.Jarenov and L.A.Gusakova, Mol.Cryst.Liq.Cryst.7, 279 (1969).

94. A. de Vries, Mol. Cryst.Liq.Cryst., 11, 361 (1970); 20, 119 (1973).

95. B.Jha and R.Paul, Proc.Nucl.Phys. Solid State Phys. Symp. India, 19c, 491 (1976).

96. H.P.Klug and L.E.Alexander, X-ray diffraction procedures for polycrystalline and amprphous materials, John Wiley and Sons, NY, ch.3 (1974).

97. C.Kittel, Int.to Solid State Phys. Wiley Eastern, Ch.2 (1976).

98. Ref. 96, pages 114 and 473.

99. Ref 96, page 308.